YOLOv8-Based Microplastic Detection and Quantification in River Water Microscopic Images

Musthofa Galih Pradana[1,*], Retno Dwi Nyamiati[2], Husna Muizzati Shabrina[3], Muhammad Adrezo[4], Nurhuda Maulana[5]

[1,4]*Data Science Department, Computer Science Faculty, Universitas Pembangunan Nasional Veteran Jakarta, Indonesia*

[2]*Chemical Engineering Department, Industrial Engineering Faculty, Universitas Pembangunan Nasional Veteran Yogyakarta, Indonesia*

[3]*Environmental Engineering Department, Mineral Technology Faculty, Universitas Pembangunan Nasional Veteran Jakarta, Indonesia*

[5]*Informatics Department, Computer Science Faculty, Universitas Pembangunan Nasional Veteran Jakarta, Indonesia*

(Received: November 5, 2025; Revised: January 10, 2026; Accepted: March 28, 2026; Available online: May 3, 2026)

Abstract

Plastic particles with various size variations such as microplastics are environmental contaminants that are widely found in waters and have the potential to cause negative impacts. The process of identifying plastic particles using microscopic imagery manually takes a lot of time and considerable cost. In order to provide an alternative solution as part of early detection, microscopic image-based plastic particle detection was carried out with the YOLOv8 architecture, accompanied by an estimate of microplastic abundance in microplastic units per cubic meter. This study aims to develop and evaluate the detection of plastic particles in microscopic images of river water. This research dataset consists of 300 microscopic images taken from three river locations in Indonesia and annotated for model training and testing. The results of the evaluation showed that the proposed model had an aggregate performance value with a precision value of 0.786, recall of 0.66, and mAP@0.5 of 0.731. Additional test results show that with the addition of image resolution, the precision value can increase to 0.804 and the value mAP@0.5 increases to 0.762, even at the expense of computing time, which is also increasing. Extended scenario-based analysis showed that more than 87% of the detected objects fell into the category of small objects, affecting the localization sensitivity and variability of the estimated MPS value. This study also validated the results of object detection with FTIR-based laboratory tests using a full quantitative agreement between the model detection results and the identification of plastic particle materials at the sampling location level. The main contribution and findings of this study is an integrated evaluation framework for object detection, particle size characterization which is expected to be an alternative to the initial screening tool for plastic particle content.

Keywords: Microplastics, YOLOv8, Object Detection, Microscopic Images, FTIR Validation

1. Introduction

Several reports state that Indonesia's waters have challenges regarding the accumulation of plastic waste, so a methodological approach is needed to be able to overcome this problem comprehensively. Based on reports and data from Environmental Science & Technology, the existence of plastic particles, specifically microplastics, is found in Indonesian waters [1]. This condition is due to the global plastic production factor which continues to increase. Data shows that in 1950 plastic production was 2 million metric tons and increased by 400 million metric tons in 2020. This will continue to increase based on predictions and there will be a doubling increase by 2040 [2]. The growth of plastic production that is increasing from year to year can have ecological effects whose impact will certainly cause many negative effects. According to some research, plastics are grouped based on size such as macroplastics, mesoplastics, microplastics, and nanoplastics, all of which fall under the category of plastic debris or particles. This plastic problem is one of the important issues. The main problem in the current condition is that rivers in Indonesia, according to the results of the Ecoton survey, have been polluted by microplastics by 98% spread across 24 provinces.

Microplastics are not only found in the water but also in household appliances such as blenders which are also found [3]. The increasing volume of plastic particles in waters such as seas and rivers and becoming new contaminants in the environment, makes it interesting to study [4] specifically in Indonesia [5] Because plastic particles become an

***Corresponding author: Musthofa Galih Pradana (musthofagalihpradana@upnvj.ac.id)**
DOI: https://doi.org/10.47738/jads.v7i2.1262

emergent contaminant that attracts global attention and various studies produce data that cannot be compared due to differences in methodology [6]. Detection of microplastics and even nanoplastics [7] can be done by utilizing artificial intelligence [8] [9] specifically, using computer vision or image processing which has many techniques and approaches [10] in detecting images [11]. The model that is usually used is the convolutional neural network model which has many architectures [12] to be able to detect images in multiple characters [13] and able to recognize various sizes, shapes, and colors of microplastics [14] which has fairly accurate results with a < deviation of 10% and a process speed of 10 seconds per image [15]. Other approaches such as Raman spectroscopic imaging [16] or with Multispectral Imaging [17]. Other research was also able to detect with a combination of IoT and CNN. One of the algorithms that can be used is CNN with VGG16 architecture with VGG16 results being able to be classified into three types: fragments, pellets, and lines [18]. Another study using a two-stage architecture (U-Net + VGG-16) succeeded in automatically counting and identifying microplastics measuring 1–5 mm with high precision and short processing time. In addition, the use of a camera or a regular mobile phone makes this method accessible and low-cost, suitable for large-scale field monitoring. Another MP-Net model with deep learning-based image segmentation successfully improved the quantification accuracy of fluorescent microplastics compared to traditional approaches [19].

Some image-based detection results such as the results of ResNet-10 to detect, classify, and perform segmentation instances of marine microplastics [20] and detection using cameras in microplastic detection with YoloV5 [21] or combination of microscope imagery under UV with Faster-R-CNN-FPN (ResNet-50) [22]. In addition, with the application of deep learning, it is able to achieve an accuracy of up to 96% [23]. In addition to an image-based approach, one of the identifications that can be done to test the content of microplastics is to predict the value of MPS units or microplastics can be done based on machine learning such as Chengzhi Liu's research [24], Shangtuo Qian [25] and Yu Zhen [26] all of which utilize artificial intelligence or machine learning such as ensemble learning [27] to see the content of existing microplastics. This approach can certainly be used to see and predict results based on real data [28]. Other results such as Random Forest to map and predict the concentration of MPs get model results of up to 86% [29] or quite optimal results [30]. A comparison of several methods of GBoost, LightGBM, CatBoost shows the best CatBoost results for predicting MPS levels in water [31]. Other models such as LS-SVM, Random Forest (RF) and LSTM are also able to predict the amount of MP in peatland sediment samples [32] or a combination of Decision Tree, RF, XGBoost [33] combination Artificial Neural Networks and Hidden Markov Models (ANN-HMM) [34]. State of the art this study detects the content of plastic particles in water by taking microscopic images such as automatic research from images [39] or data electron micrographs [40] where the model used applies convolutional neural networks with good accuracy to several models [41] [42]. This study will detect images containing microplastics and calculate the microplastic content (MPS) in the image. Then the detection and prediction results will be validated by test results from the laboratory to ensure the validity of the test data-based results using FTIR analysis to confirm the plastic polymer particles in the sample being studied.

This research is expected to be able to cover some of the weaknesses of previous research that still focuses on visual detection related to the content of plastic particles without standardized validation. This study attempts to propose an integrated framework in detecting and estimating the amount of plastic particle content in microscopic images. The main contributions of this study are (1) plastic particle detection model in microscopic images of river water samples, (2) pixel-to-micrometer caliphs in plastic particle size estimation, (3) prediction of plastic particle size in MPS units, and (4) validation of plastic particle detection and prediction results by FTIR analysis tested in the laboratory. This approach is expected to provide a solution in cutting the long flow of laboratory tests and become an initial screening tool for plastic particle pollution in rivers with a scenario-based approach for the detection and analysis of plastic particles. The study not only focused on evaluating model performance, but also investigating the relationship of bounding box size, prediction variability and microscopic image characteristics with the stability of MPS estimates. This research is expected to be able to make a scientific contribution by not only focusing on detection accuracy but also presenting scenario-based reflective analysis. Studies are generally based on classification and detection without any correlation with quantitative estimation of the abundance of plastic particles and based on no evidence of FTIR analysis.

2. Literature Review

2.1. Related Works

Several relevant studies on plastic particle detection are focused on three main categories, namely: (1) computer vision-based plastic particle detection, (2) prediction of plastic particle size estimation with artificial intelligence, and (3) validation of plastic particle detection results by laboratory analysis. This is important considering the significant

growth in plastic production and starting to pollute river ecosystems in particular. So that the development of detection models is an urgency that continues to be researched by several previous researchers. Manual detection of plastic particles carries out a fairly long laboratory-based identification and analysis. The long and time-consuming scientific mechanism for detecting plastic particles creates a research gap that can be overcome with computer vision models. The model that has good accuracy and object detection capabilities is Convolutional Neural Networks (CNN).

CNN have one of the architectures that has good detection characteristics, namely by using YOLO. The results of CNN-based research with YOLO architecture have good results such as studies that achieve high accuracy of 98% [35]. The advantages of YOLO with its model variety have advantages in inference speed and ease of implementation. Previous research on plastic particle detection used YOLO's one-stage architecture with a focus on accuracy metrics such as precision, recall and mAP, and has not touched on model behavior on small objects. This research will try to cover the gap in evaluation research on the sensitivity of small objects that will be tested in this study. The detection of plastic particle objects will be combined with the prediction of the value of microplastics per cubic meter (MPS). The model in this study will measure the value of plastic particles in objects. In practice, the mean particle size (mean micrometer) does not directly affect the MPS calculation. This identification puts the identification of particles with MPS estimation as additional information for the initial quantitative component in the analysis of plastic particles. This research still has limitations where these results are still an initial model and need further development.

The results of object detection and MPS size identification were the two main outputs of the study. In order to ensure and validate that the detected plastic particles are correct and precise, a chemical analysis is carried out with Fourier Transform Infrared Spectroscopy (FTIR) as a material for validating the results. The Fourier Transform Infrared Spectroscopy analysis position is used for validation parameters, because the analysis size in FTIR is a reference value that shows credibility. Although Fourier Transform Infrared Spectroscopy has good results, this analysis has a drawback, namely the long analysis time, the high cost so that this detection model is expected to be able to be a solution and contribution to technological innovation.

2.2. Comparative Analysis and Research Gap

A structured comparison based on the results of a literature review of several existing approaches to object detection models that have been carried out will be summarized in table 1. This will be used in the analysis based on the selection of the type of architecture in the table 1.

Table 1. Comparative Model

Model	Detection Type	Small Object Capability	Speed	Annotation Need	Strengths
Faster R-CNN [36]	Two Stage	High	Slow	Bounding Box	Strong Localization
SSD [37]	Single Stage	Moderate	Fast	Bounding Box	Efficient Inference
YOLOv5 [38]	Single Stage	Moderate	Very Fast	Bounding Box	Lightweight and Stable
YOLOv8 [39]	Single Stage	High	Fast	Bounding Box	Improved Feature Aggregation and Training Stability

Table 1 showing comparative results has their own advantages and limitations. Based on the detection type, there are two types, namely single, and double stage. The advantages of single stage are in terms of balance of speed and accuracy, this is relevant to the data that will be used in this study. The annotation bounding box model with high small object capability characteristics shows that the YOLOv8 model is relevant to small particles and image characters that have low contrast to the background. Some of the results of previous studies focused on detection accuracy without considering several aspects such as the influence of particle size and distribution. This is the main contribution in this study is the YOLOv8-based object detection methodological framework with chemical laboratory test validation, so that the results become more comprehensive. Some of these deep learning-based techniques are able to detect and classify plastic particles with microscopic image media. On average, the model used uses Convolutional Neural Networks (CNN) due to its ability to extract good visual features. Then, segmentation such as U-Net or MP-Net provides more precise spatial details at the pixel level, which is relevant in the separation of plastic particles from the background. On the other hand, YOLO or Faster R-CNN's bounding box-based detection has strong object localization capabilities, although it takes a long inference time. The biggest challenge in detecting plastic particles is the small size

of the object, which will be relevant to the YOLOv8 model which has a better feature aggregation mechanism, and has qualified training stability.

3. Methodology

This study is an experimental study based on microscopic image data. In addition to the process of detecting plastic particles in water. This methodology is prepared in an integrated manner starting from sampling from the river, developing datasets, detection and analysis of results.

3.1. Study Area, Sample Collection and Image Acquisition

River water samples were taken from three locations in Yogyakarta, Indonesia. The selection of location takes into account the location, geographical aspects, and human activities around the river in order to vary the distribution of plastic particles. Samples from this river water are processed in the laboratory through filtration and preparation stages according to standard analysis procedures. The image data used in this study used microscopic images from river water sampling for laboratory testing. The sample observation device uses a binocular stereo microscope with an optical tilt angle of 45°, an interpupillary range of 55–75 mm and lighting with a halogen lamp of 12 V. The reason for the selection of this is to produce good and adequate visualization of plastic particles, because plastic particles are small. All image data uses one uniform resolution of 1200 x 1600 pixels with all the same configuration. This is done to ensure the consistency of the spatial and visual scale. The parameters used for microscopic image data collection are focus settings, lighting intensity, and the distance of objects to the lens. This uniformity and similarity is expected to be able to provide a reliable analysis to explore the relationship between microscopic image characteristics and the distribution of bounding box size and model prediction variability. In the next process, the data will be used as input data for the annotation and model development process.

3.2. Dataset Construction Annotation and Preprocessing

The total dataset used was 300 microscopic images after going through the image acquisition stage. The detailed information is as many as 1,701 instances of plastic particles. The number of images is still relatively limited, the characteristics of this dataset have an object density that allows the model to be able to study visual patterns in a representative manner without depending on the size of the dataset. The process is carried out by identifying the bounding box on the identified plastic particles. The process regarding the dataset, the data is divided into three subsets, namely training data of 70%, validation data of 20% and testing data of 10%. The data sharing is done randomly with the aim of ensuring that the distribution of the image remains proportional and can reduce the possibility of bias and improve the generalization capabilities of the model. In order to increase data diversity and avoid the risk of overfitting, the augmentation process is carried out with a rotation approach, horizontal and vertical flipping, translation, rescale, brightness and contrast adjustment. This is done to provide a variety of visual conditions without changing the characteristics of microscopic data in plastic particles. The application of data augmentation techniques to increase the variability of the dataset, in addition to increasing the resistance of the model to scale and particle variations. Augmentation becomes a standard procedure, not an independent experimental variable, so it does not include a separate analysis. The data used were 300 microscopic images with a total of 1701 instances that had been annotated. This is admittedly quite limited for a model training.

Therefore, the training process uses weight-based transfer learning on the YOLOv8 model. This approach is expected to be able to take advantage of visual features and can be adapted into plastic particle detection, so that the data is sufficient to train the model while maintaining the generalization capabilities of the model. Bounding box annotations are performed based on visual inspection of microscopic images. The control procedure is carried out by reviewing annotations and verifying through the particle labeling inspection process. This approach is adequate for the purpose of detecting single-class plastic particles with relatively homogeneous characteristics in microscopic images. The dataset was divided into training, validation and testing using a 70:20:10 ratio. Divisions are done at the image level, ensuring that each image appears only in one subset. This approach prevents data leakage that can occur if individual object instances of the same image are distributed to various randomly executed subsets, to ensure each subset has a representative variation. This limited amount of data is trained and annotated using transfer learning. The results show that the model has stable convergence, this means that this dataset is sufficient for the detection task of single-class objects. With dataset conditions predominantly small objects, no explicit reweighting is performed, but the model relies on multi-scale feature learning that affects resilience.

3.3. Spatial Calibration and Particle Size Estimation

The spatial calibration process was carried out in the study to convert the particle size from the pixel unit to the physical unit (micrometer). This process is done by using 40 magnifications. Repeated measurements resulted in a configuration applied to this study with a "40× magnification, the image calibration yielded a spatial resolution of about 2.0 µm per pixel. This is the dimension of the bounding box detected to calculate the size of plastic particles in micrometers and will be applied in the analysis of size distribution and interpretation of plastic particle values. The conversion factor is based on the level of optical magnification, the resolution of the camera sensor. The configuration result of 2.0 µm per pixel represents the ratio between the physical length of the object in the microscope's field of view compared to the number of pixels in the digital image. Meanwhile, recording calibration uncertainty can affect the estimated size of plastic particles. With the process of calculating the abundance of plastic particles in MPS units, small variations in the calibration factor affect the estimation of the absolute size of the particles. Spatial calibration is done to convert pixel-based measurements into real-world dimensions. The calibration factor is determined using a reference scale of known physical length, taken under the same microscope configuration as the sample image with reference:

$$S = \frac{L\ Real}{L\ Pixel} \tag{1}$$

Based on this procedure, a conversion factor of 2.0 µm per pixel is obtained. The calibration is still possible due to the uncertainty arising from image resolution and optical conditions which are limitations. The model will be developed to detect objects using CNN with the YOLOv8 architecture. This architecture uses a single-stage object detection approach. The reason for choosing the model is because it has a good ability to detect small and dense objects, this is relevant to the characteristics of the data used, namely plastic particle data in microscopic images. The model was used to detect one class of objects by training using the Ultralytics YOLOv8 framework for 100 epoch and applying the ADAM optimizer, with an initial learning rate of 0.001 and a batch size of 16. The selection of the ADAM optimizer was based on adaptive training rates and convergence stability, which is very relevant to the data in this study which is not very large and has heterogeneous visual characteristics. The model used is the YOLOv8n (nano) architecture due to its lightweight structure and compatibility with the characteristics of the dataset. The model is trained by utilizing feature representations to be able to increase convergence during training. Optimization in YOLOv8 is based on the composite loss function in the integration of localization classification and object detection with the formulation of:

$$L = L_{cls} + L_{box} + L_{obj} \tag{2}$$

3.4. Scenario-Based Evaluation and Performance Metrics

Model performance is evaluated based on standard metrics such as recall, precision, and mAP. This metric is used to analyze the behavior of an object model that has variations. Where the focus is on the detection of objects with various particle sizes and spatial distribution in microscopic images. The evaluation is also based on standard object metrics below a predetermined threshold. A threshold of 0.25 is applied to filter the bounding box that will be predicted and ensure a sufficient level of confidence. The other value is that the Intersection over Union (IoU) limit for mAP50 is set at 0.5, while mAP50–95 is calculated at the IoU threshold range from 0.5 to 0.95 in a step of 0.05, following standard evaluation practices in object detection. This is done as a framework to ensure reliable performance detection. The model is evaluated using object detection metrics. Precision describes the ratio of correctly detected objects, recall indicates correct detection to ground-truth. The gauges follow the standard COCO evaluation protocol. The YOLOv8 model is not only lightweight, but also relevant and suitable for small datasets and single classes. With larger variants and size of resources, it can be done as part of the improvement and sustainability of research. The selection of a sample of 39 samples was selected using graded sampling based on particle size, to ensure the representation of small, medium, and large objects. This analysis is exploratory due to the limited sample size.

3.5. Microplastic Abundance Estimation (MPS) and FTIR Validation

The calculation of the value of plastic particles is carried out by applying the microplastic per cubic meter (MPS) metric which is used as a ratio of the number of detected plastic particles to the volume of water. Standardization is carried out to maintain freshness by using a water volume of 100 m^3. Apart from the prediction process carried out, there is a validation stage based on Fourier Transform Infrared Spectroscopy (FTIR) as a stage to validate the existence of plastic particles by strengthening the relevance of image-based detection results that will be positioned as an initial screening tool. The measurement of microplastic abundance is calculated as follows:

 ISSN 2723-6471

$$MPS = \frac{N}{V} \quad (3)$$

The MPS calculation estimate assumes that the particles detected in the microscopic image represent the distribution of particles in units of water volume in the sample. The use of this estimate does not take into account the potential sampling bias which is a limitation of the approach carried out. The process of converting the output of an object into an MPS, requires a computational workflow. This flow will combine bounding box detection with MPS estimation. The sequence of steps consists of: Object detection, bounding box extraction, spatial calibration, particle size estimation and MPS value estimation. Microscopic image data will be processed in the YOLOv8 model with the identification of plastic particles. The objects detected by the model will be represented in bounding boxes based on the central coordinates and dimensions in pixels. The use of width and height on the bounding box is used to calculate the size of the dominant plastic particles in the image. The process of converting pixels to real dimensions is carried out spatial calibration using the following microscope calibration:

$$S = 2.0\ \mu m/pixel \quad (4)$$

The predicted particle size in micrometers is calculated as:

$$di = pi\ \times\ s \quad (5)$$

MPS calculation is the ratio between the number of detected particles and the volume of water sampled (MPS = N/V).

4. Results and Discussion

The results and discussion section will present the results of several experiments conducted based on scenarios to explore and obtain information on the evaluation of the performance of plastic particle detection, predictive stability results, as well as the relationship between the characteristics of microscopic images and the size of the bounding box and the estimated calculation of the value of plastic particles in MPS units. The data and analysis presented emphasize the understanding of the variability and limitations produced by microscopic image-based data-based predictions.

4.1. Characteristics of Microscopic Datasets

The characteristics and visualization of the microscopic image dataset in this research data which shows variations in the density of objects. In addition, on Figure 1 showing microscopic image data accompanied by a bounding box on plastic particles.

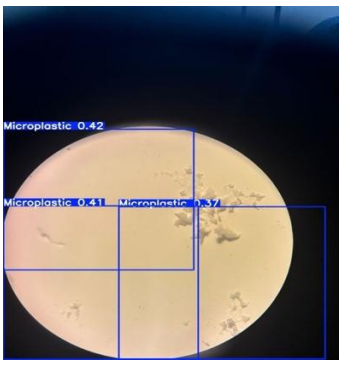

Figure 1. Object Detection

These variations can contribute to differences in localization quality and prediction stability, which will be further discussed in the analysis of bounding box distribution and MPS variability.

4.2. Particle Plastic Object Detection Performance

The YOLOv8 model in detecting objects has a performance by showing a precision value of 0.786. The recall value is 0.66, mAP@0.5 is 0.731 and the value is mAP@0.5-0.95 with a value of 0.346. The precision value obtained is quite relatively high which indicates that most of the objects detected in the model are indeed plastic particles. This high precision value has a good meaning, but on the other hand the recall value is still quite low showing that many particles

ISSN 2723-6471

fail to be detected, especially in high-density images with very small particle sizes. The performance evaluation of the YOLOv8 model showed a precision value of 0.786, a recall of 0.66, a mAP@0.5 of 0.731, and a mAP@0.5–0.95 of 0.346. The relatively high precision value indicates that most of the objects detected are true microplastic particles. However, lower recall values indicate that there are still undetected particles, especially in high-density images and very small particles. This result is reinforced by the precision recall curve on Figure 2.

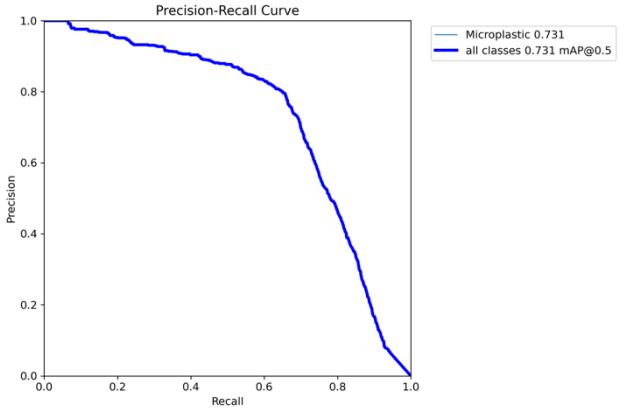

Figure 2. Precision-Recall Curve

The results of this curve provide an overview of the behavior of the YOLOv8 model at various levels of detection completeness. The model as a whole is able to maintain a fairly high precision value with the precision of the detection object. However, on the other hand, on the other hand, there is a sharp decrease in precision values. An indication of this pattern is the ability to detect objects with very small particles overlapping each other. This is relevant to the characteristics of microscopic image data where there are many small and transparent objects. This evaluation is based on aggregate metrics with reference to precision, recall, mAP@0.5 and mAP@0.5–0.95 values. The details of the results are shown on Table 2.

Table 2. Testing Model

Category	Value
Images	300
Instances	1701
Box P	0.786
R	0.66
mAP50	0.731
mAP50-95	0.346

The results of the evaluation summarize an evaluation based on metric aggregate which provides an overview of detection accuracy, but only limited to general performance regarding object detection. These results do not fully reflect the differences in image conditions, object density, small particle dominance and do not explain the factors that affect the results of location quality and prediction stability, so a more in-depth scenario-based analysis is needed to examine the distribution of bounding box size and prediction variability referring to microscopic image characteristics. Further analysis as an additional study will be discussed in this study to obtain more comprehensive results. Higher image resolution has the opportunity to improve detection detail even though it is aligned with increased computational costs and inference time. A more detailed analysis can be a suggestion for research development.

4.3. Analysis Based on Scenario

The results of the metric aggregate-based evaluation provide information about the detection performance of the YOLOv8 model. These results need to be strengthened by scenario-based analysis by identifying factors that affect the localization quality and prediction stability in microscopic images. This additional analysis will examine additional information in the form of the relationship between the distribution of bounding box size, visual characteristics of the image, and prediction variability in the estimation of the mps value. The analysis that can be done is the distribution of

the bounding box area where the results show that the majority of detected objects are in the category of small size. The total bounding box was 39 as an analysis sample, around 87.17% was included in the small category with a median value of 0.00175 and an average value of 0.00658 which was quite relative to the image dimension. Scenario-based analysis using 39 bounding boxes was selected to represent different categories of particle sizes and observed conditions. The goal is exploratory, where information on the distribution of bounding box size distribution, prediction variability can be explored further. The dominance of bounding box distribution, which falls into this small category, has implications for the quality of localization. This influence will be significant in localization errors that cause a decrease in the value of Intersection over Union (IoU). This is clearly evident from the results of the significant difference in the values of mAP@0.5 and mAP@0.5-0.95. Another analysis is the prediction variability and estimation stability in predicting the value of plastic particle content with MPS units by comparing the density of microscopic image objects. The results of this analysis are shown in Table 3.

Table 3. Variability of Prediction and MPS

Density	Total Particles	MPS	Mean Area	Std Area
Low	8	0.08	0.21019	0.006607
Medium	12	0.12	0.005356	0.005818
High	19	0.19	0.001276	0.001437

The results of the analysis showed that the MPS value increased as the density of the object was shown between the total particles and MPS columns. The increase in the MPS value was accompanied by a significant decrease in the average area of the bounding box area. Meanwhile, the standard deviation value shows that objects with high density have a smaller standard deviation value compared to objects that have low density values. The indication of the results shows that the detected objects tend to be homogeneous in size with large quantities. This means that the estimated stability of MPS is not only determined by the number of detected particles, but also by the distribution of the size and structure of the object. These results also explain the difference in precision and recall values in the evaluation of aggregate metrics, where small objects dominate with high object density values so that there is a probability of possible missed objects (false negative). MPS level classification with the following references: Low density: MPS $\leq$ 0.10 particles/m³, Medium density: 0.10 < MPS $\leq$ 0.15 particles/m³, High density: MPS > 0.15 particles/m³. This is based on the empirical distribution of the dataset where the observed values range from 0.08 to 0.19 particles/m³. Scenario-based subset assessment was carried out by conducting a statistical comparison of 39 bounding boxes selected from 1,701 instances. It is based on the particle size distribution. As in the results of the Table 4 shows that the comparable value is at 45.2 pixels with a consistent standard deviation at (19.4 and 18.7 pixels). The distribution of small particles (<50 pixels) dominated with complete datasets (86.8%) and (84.6%). This states that the subset captures the dominant characteristics of the dataset, specifically small particles and objects. These findings corroborate that despite the limited size, the selected subset is able to reflect the size of the particles in the dataset.

Table 4. Scenario Subset

Metric	Full Dataset	Scenario Subset
Mean Particel Size (pixel)	43.7	45.2
Standard Deviation (pixel)	19.4	18.7
Small Particles (<50 px)	86.8%	84.6%
Medium Particles (50-100 px)	10.5%	12.8%
Large Particles (>100 px)	2.7%	2.6%

4.4. Discussion on Small Object Detection

The dominance of small objects in the dataset of 87% is the main challenge in the detection of plastic particles. This section will examine the effect of spatial resolution on the performance of model detection. Additional experiments were conducted using different model input resolutions while still using the same training configuration. This change in input resolution is only made to the pre-processing model which has no direct effect on the resolution of the original image and the main calibration. The results of the experiment are shown in detail on Table 5.

ISSN 2723-6471

Table 5. Performance Model

Configuration	Precision	Recall	mAP50	mAP50-95	Inference Time
640 x 640 (baseline)	0.786	0.660	0.731	0.346	18 ms
1024 x 1024	0.804	0.712	0.762	0.401	35 ms

An additional scenario in the test results with different input resolutions, was proven to increase the precision value at 0.804. Another improvement also occurred in the recall value, mAP50, mAP50-95. This performance improvement indicates that higher input resolution allows the model to retain spatial data. However, this improvement also increases the computational time in the inference process. It can be concluded that, there is a trade-off between detection accuracy and computational efficiency. Based on the results of the table, it can be further analyzed about the consistent patterns where the dominance of small particles and the variability are prominent. With a small bounding box size, it is more sensitive to localization errors. This can affect greater IoU variability. Further observations could be more comprehensive testing in follow-up research. This refers to variations in IoU and trust scores. Where is the descriptive measure used. The comparison made illustrates the different processing scales between the image level and the sample level. This is not a direct similarity, the use of the method used functions as a quick filter, while the FTIR method provides a more in-depth analysis, so it is expected to complement each other.

4.5. Validation of Model with Laboratory Test

The combination of quantitative agreement analysis and characterization with FTIR shows that YOLOv8-based plastic particle detection can be used as an initial screening tool for the detection of the presence of plastic particles in water. This validation complements the aggregate metrics-based evaluation and scenario-based analysis. The results of the previous analysis need to be strengthened again by validating the model prediction and the results of laboratory tests with FTIR. The metric used for evaluation deals is the Binomial Confidence Interval. This metric is proposed with the concept that if plastic particles are detected by the model, it will be confirmed by the results of chemical laboratory tests with FTIR. The number of samples is 3 river water samples or 3 location points. Thus, the values k = 3, and n = 3 with an agreement level value of 1 because all locations detected plastic particles.

The next step is to calculate a confidence interval of 95% using Clopper-Perason Exact which is relevant for small and binary-type data. The value of the confidence interval has α=0.05. Advanced measurement with a positive predictive value (PPV) value with a value of 100. Value of overall agreement, sensitivity, Positive Predictive Value and Upper Bound is 100, and the lower bound is 29. The meaning of the results in the table is from the confidence level of 95% of the reliability value, the observation results at 3 location points are produced a lower bound value of 29% and an upper bound value of 100%. This shows that although the agreement value shows a perfect value, the performance probability can vary due to the limitation of river water test samples which are only 3 location points, so that the interval values produced by the lower bound and upper bound are quite wide. The addition of a sample location point could be a suggestion in the future. However, this is a value agreement that reflects the model's ability as a plastic particle screening tool, not as a full substitute for laboratory characterization. The results of this binominal validation do have small sample limitations, due to many factors that are obstacles in the validation of the results. However, this limitation can be addressed because this wide interval reflects the reliability of statistical inference which is limited to small samples, so agreement is made as part of the evidence. The results of the three locations showed that the particles detected by the model were plastic particles with FTIR results as a validation reinforcement with detailed polymer characteristics, Location 1 have characteristics Polyvinylidene fluoride (PVDF), Location 2 have Ethylene–acrylic acid (EAA) copolymer and Location 3 have High-density polyethylene (HDPE). The results of the proposed microscopic image detection model have a fast inference time in the range of 18-35 ms. In comparison to conventional FFID, it generally takes about 30-60 minutes per sample.

The difference in processing time between these two methods can be interpreted by the image detection model can be positioned as the initial stage for the identification of the presence of plastic particles in water. The method is not intended as a substitute for FTIR because it is still necessary for the chemical identification of polymer composition. This proposed method has the potential to be used as a screening stage to help the preliminary process more effectively. Validation using FTIR was carried out to confirm the plastic particles detected in the model. This validation is done at the sample level, not the sat uke correspondence between bounding boxes. So the validation carried out is used to match that the detected object is indeed proven to contain plastic particles. The validation process applies a binomial

confidence interval (Clopper–Pearson), assuming a binomial distribution of success during the experiment. Due to the small sample size (n = 3), the interval was wide and the results were interpreted as preliminary evidence.

5. Conclusion

This study shows that YOLOv8-based plastic particle detection with microscopic data achieves good aggregate performance with a precision value of 0.786 and a value of mAP@0.5 of 0.731, although there are still challenges regarding the quality of localized bounding boxes. Scenario-based analysis showed that the dominance of small objects reached 87% which directly affected the localization performance and the variability of the calculation estimation of plastic particles. Additional test results show that with the addition of image resolution, the precision value can increase to 0.804 and the value mAP@0.5 increases to 0.762, even at the expense of computing time. Laboratory validation used with FTIR showed full quantitative agreement between predictions using location-based models. Although the study still has limitations on the sample size of the site which affects the model's generalization ability on the environmental conditions of the river or different model configurations. This study still has limitations in the size of the dataset as well as the number of samples, so it has limitations in the generalization of the model, therefore the follow-up research suggests to expand the location point and improve the detection ability of objects in microscopic images.

6. Declarations

6.1. Author Contributions

Conceptualization: M.G.P., R.D.N., H.M.S., M.A., and N.M.; Methodology: R.D.N.; Software: M.G.P.; Validation: M.G.P., R.D.N., and N.M.; Formal Analysis: M.G.P., R.D.N., and N.M.; Investigation: M.G.P.; Resources: R.D.N.; Data Curation: R.D.N.; Writing Original Draft Preparation: M.G.P., R.D.N., and N.M.; Writing Review and Editing: R.D.N., M.G.P., and N.M.; Visualization: M.G.P.; All authors have read and agreed to the published version of the manuscript.

6.2. Data Availability Statement

The data presented in this study are available on request from the corresponding author.

6.3. Funding

We would like to thank the Directorate of Research, Technology, and Community Service (DRTPM) of the Ministry of Higher Education, Science and Technology, for the funding support of this research under the Fundamental Regular (PFR) scheme, Universitas Pembangunan Nasional Veteran Jakarta, Universitas Pembangunan Nasional Veteran Yogyakarta and all colleagues for their valuable assistance.

6.4. Institutional Review Board Statement

Not applicable.

6.5. Informed Consent Statement

Not applicable.

6.6. Declaration of Competing Interest

The authors declare that they have no known competing financial interests or personal relationships that could have appeared to influence the work reported in this paper.

References

[1] Cornell University, "Study maps human uptake of microplastics across 109 countries," *Cornell Chronicle*, May 2024. [Online]. Available: https://news.cornell.edu/stories/2024/05/study-maps-human-uptake-microplastics-across-109-countries

[2] Research Department, "Annual production of plastics worldwide from 1950 to 2022," Statista, Jan. 25, 2023. [Online]. Available: https://www.statista.com/statistics/282732/global-production-of-plastics-since-1950/

[3] Y. Luo, O. S. Awoyemi, R. Naidu, and C. Fang, "Detection of microplastics and nanoplastics released from a kitchen blender using Raman imaging," *J. Hazard. Mate*r., vol. 453, no. Jul., pp. 1–12, 2023, doi: 10.1016/j.jhazmat.2023.131403.

[4] A. Tarafdar, S.-H. Choi, and J.-H. Kwon, "Differential staining lowers the false positive detection in a novel volumetric measurement technique of microplastics," *J. Hazard. Mater.*, vol. 432, no. Jun., pp. 1–12, 2022, doi: 10.1016/j.jhazmat.2022.128755.

[5] A. Priyanto, D. A. Hapidin, D. Edikresnha, M. P. Aji, and K. Khairurrijal, "Predicting microplastic quantities in Indonesian provincial rivers using machine learning models," *Sci. Total Environ.*, vol. 961, no. Jan., pp. 1–12, 2025, doi: 10.1016/j.scitotenv.2025.178411.

[6] L. Lv, "Challenge for the detection of microplastics in the environment," *Water Environ. Res.*, vol. 93, no. 1, pp. 5–15, 2021, doi: 10.1002/wer.1281.

[7] A. Nene, "Recent advances and future technologies in nano-microplastics detection," *Environ. Sci. Eur.*, vol. 37, no. 1, pp. 1–12, 2025, doi: 10.1186/s12302-024-01044-y.

[8] P. Guo, Y. Wang, P. Moghaddamfard, W. Meng, S. Wu, and Y. Bao, "Artificial intelligence-empowered collection and characterization of microplastics: a review," *J. Hazard. Mater.*, vol. 471, no. Jun., pp. 1–12, 2024, doi: 10.1016/j.jhazmat.2024.134405.

[9] H. Jin, F. Kong, X. Li, and J. Shen, "Artificial intelligence in microplastic detection and pollution control," *Environ. Res.*, vol. 262, no. Dec., pp. 1–12, 2024, doi: 10.1016/j.envres.2024.119812.

[10] D. Arisandi, A. Khoerunnisa, R. Subekti, A. E. Setiawan, and C. Ramdani, "Performance evaluation of CLAHE-enhanced edge detection on low-light faces," *J. Comput. Innov. Emerg. Technol.*, vol. 1, no. 1, pp. 7–10, 2025, doi: 10.64472/jciet.v1i1.2.

[11] B. Hu, "Using artificial intelligence to rapidly identify microplastics pollution and predict microplastics environmental behaviors," *J. Hazard. Mater.*, vol. 474, no. Aug., pp. 1–12, 2024, doi: 10.1016/j.jhazmat.2024.134865.

[12] M. G. Pradana, H. Khoirunnisa, and I. W. R. Pinastawa, "Evaluation of convolutional neural network model architecture performance," *Int. J. Informatics Multimed. Cyber Inf. Syst.*, vol. 2023, no. Jan., pp. 628–632, 2023, doi: 10.1109/ICIMCIS60089.2023.10349075.

[13] D. R. Maulana, M. G. Pradana, and M. P. Muslim, "Handwriting classification of Sundanese script using LBP feature extraction and CNN," *Int. J. Informatics Multimed. Cyber Inf. Syst.*, vol. 2024, no. Nov., pp. 1079–1084, 2024, doi: 10.1109/ICIMCIS63449.2024.10956206.

[14] M. D. A. Hasan, K. Balasubadra, G. Vadivel, N. Arunfred, M. V. Ishwarya, and S. Murugan, "IoT-driven image recognition for microplastic analysis in water systems using convolutional neural networks," *Int. J. Comput. Commun. Control*, vol. 2024, no. Feb., pp. 1–6, 2024, doi: 10.1109/IC457434.2024.10486490.

[15] M. Giardino, V. Balestra, D. Janner, and R. Bellopede, "Automated method for routine microplastic detection and quantification," *Sci. Total Environ.*, vol. 859, no. Feb., pp. 1–12, 2023, doi: 10.1016/j.scitotenv.2022.160036.

[16] K. Liu, X. Pang, H. Chen, and L. Jiang, "Visual detection of microplastics using Raman spectroscopic imaging," *Analyst*, vol. 149, no. 1, pp. 161–168, 2024, doi: 10.1039/D3AN01270K.

[17] D. Ho and H. Feng, "Shedding light on the polymer's identity: microplastic detection and identification through Nile red staining and multispectral imaging (FIMAP)," *J. Environ. Chem. Eng.*, vol. 2025, no. Feb., pp. 1–12, 2025, doi: 10.1016/j.jece.2025.117944.

[18] J. Lorenzo-Navarro, "Deep learning approach for automatic microplastics counting and classification," *Sci. Total Environ.*, vol. 765, no. Apr., pp. 1–12, 2021, doi: 10.1016/j.scitotenv.2020.142728.

[19] H. Park, "MP-Net: deep learning-based segmentation for fluorescence microscopy images of microplastics isolated from clams," *PLoS One*, vol. 17, no. 6, pp. 1–12, 2022, doi: 10.1371/journal.pone.0269449.

[20] X.-L. Han, N.-J. Jiang, T. Hata, J. Choi, Y.-J. Du, and Y.-J. Wang, "Deep learning based approach for automated characterization of large marine microplastic particles," *Mar. Environ. Res.*, vol. 183, no. Jan., pp. 1–12, 2023, doi: 10.1016/j.marenvres.2022.105829.

[21] M. A. B. Sarker, M. H. Imtiaz, T. M. Holsen, and A. B. M. Baki, "Real-time detection of microplastics using an AI camera," *Sensors*, vol. 24, no. 13, pp. 1–12, 2024, doi: 10.3390/s24134394.

[22] T. Thammasanya, S. Patiam, E. Rodcharoen, and P. Chotikarn, "A new approach to classifying polymer type of microplastics based on Faster-RCNN-FPN and spectroscopic imagery under ultraviolet light," *Sci. Rep*., vol. 14, no. 1, pp. 1–12, 2024, doi: 10.1038/s41598-024-53251-5.

[23] S.-J. Royer, H. Wolter, A. E. Delorme, L. Lebreton, and O. B. Poirion, "Computer vision segmentation model deep learning for categorizing microplastic debris," *Front. Environ. Sci*., vol. 12, no. Jul., pp. 1–12, 2024, doi: 10.3389/fenvs.2024.1386292.

[24] C. Liu, "Machine learning-driven QSAR models for predicting the cytotoxicity of five common microplastics," *Toxicology*, vol. 508, no. Nov., pp. 1–12, 2024, doi: 10.1016/j.tox.2024.153918.

[25] S. Qian, X. Qiao, W. Zhang, Z. Yu, S. Dong, and J. Feng, "Machine learning-based prediction for settling velocity of microplastics with various shapes," *Water Res*., vol. 249, no. Feb., pp. 1–12, 2024, doi: 10.1016/j.watres.2023.121001.

[26] Y. Zhen, L. Wang, H. Sun, and C. Liu, "Prediction of microplastic abundance in surface water of the ocean and influencing factors based on ensemble learning," *Environ. Pollut.*, vol. 331, no. Aug., pp. 1–12, 2023, doi: 10.1016/j.envpol.2023.121834.

[27] J. Li, Z. Jiang, L. Shu, X. Li, C. Wang, and H. Zhang, "Machine learning models for forecasting microplastic dynamics in China's coastal waters," *J. Hazard. Mater*., vol. 494, no. Aug., pp. 1–12, 2025, doi: 10.1016/j.jhazmat.2025.138797.

[28] Y. Qiu, Z. Li, T. Zhang, and P. Zhang, "Predicting aqueous sorption of organic pollutants on microplastics with machine learning," *Water Res*., vol. 244, no. Oct., pp. 1–12, 2023, doi: 10.1016/j.watres.2023.120503.

[29] X. Jin, "Quantitative assessment on the distribution patterns of microplastics in global inland waters," *Commun. Earth Environ*., vol. 6, no. 1, pp. 1–12, 2025, doi: 10.1038/s43247-025-02320-2.

[30] U. Ihezukwu, C. Charoenpong, and S. Chotpantarat, "Machine learning-driven analysis of soil microplastic distribution in the Bang Pakong watershed, Thailand," *Environ. Pollut.*, vol. 375, no. Jun., pp. 1–12, 2025, doi: 10.1016/j.envpol.2025.126346.

[31] M. A. M. Reshadi, "Assessment of environmental and socioeconomic drivers of urban stormwater microplastics using machine learning," *Sci. Rep*., vol. 15, no. 1, pp. 1–12, 2025, doi: 10.1038/s41598-025-90612-0.

[32] H.-T. Tran, "Machine learning approaches for predicting microplastic pollution in peatland areas," *Mar. Pollut. Bull*., vol. 194, no. Sep., pp. 1–12, 2023, doi: 10.1016/j.marpolbul.2023.115417.

[33] A. Z. Fazil, D. D. S. Dhawala Wijeratna, and P. I. A. Gomes, "Predicting microplastic transport in open channels with different bed types and river regulation with machine learning techniques," *Environ. Pollut*., vol. 384, no. Nov., pp. 1–12, 2025, doi: 10.1016/j.envpol.2025.126912.

[34] R. I. Sajan, M. Manchu, C. Felsy, and M. J. Kavitha, "Microplastic predictive modelling with the integration of artificial neural networks and hidden Markov models (ANN-HMM)," *J. Environ. Health Sci. Eng*., vol. 22, no. 2, pp. 579–592, 2024, doi: 10.1007/s40201-024-00920-2.

[35] H. Moussaoui, "Enhancing automated vehicle identification by integrating YOLO v8 and OCR techniques for high-precision license plate detection and recognition," *Sci. Rep*., vol. 14, no. 1, pp. 1–12, 2024, doi: 10.1038/s41598-024-65272-1.

[36] J. Xu, H. Ren, S. Cai, and X. Zhang, "An improved faster R-CNN algorithm for assisted detection of lung nodules," *Comput. Biol. Med.*, vol. 153, no. Feb., pp. 1–12, 2023, doi: 10.1016/j.compbiomed.2022.106470.

[37] E. N. Yilmaz and T. S. Navruz, "Real-time object detection: a comparative analysis of YOLO, SSD, and EfficientDet algorithms," *Int. J. Hum.-Comput. Interact. Optim. Robot. Appl.*, vol. 2025, no. May, pp. 1–9, 2025, doi: 10.1109/ICHORA65333.2025.11017287.

[38] Z. Li, C. Pang, C. Dong, and X. Zeng, "R-YOLOv5: a lightweight rotational object detection algorithm for real-time detection of vehicles in dense scenes," *IEEE Access*, vol. 11, no. Jan., pp. 61546–61559, 2023, doi: 10.1109/ACCESS.2023.3262601.

[39] R. Varghese and S. M., "YOLOv8: a novel object detection algorithm with enhanced performance and robustness," *Int. J. Adv. Data Eng. Intell. Comput. Syst.,* vol. 2024, no. Apr., pp. 1–6, 2024, doi: 10.1109/ADICS58448.2024.10533619.